JOURNAL OF VIROLOGY, Nov. 2009, p. 10857–10868 Vol. 83, No. 21
0022-538X/09/$12.00 doi:10.1128/JVI.01191-09

Bimolecular Complementation of Paramyxovirus Fusion and Hemagglutinin-Neuraminidase Proteins Enhances Fusion: Implications for the Mechanism of Fusion Triggering▽†

Sarah A. Connolly,[1,2] George P. Leser,[2] Theodore S. Jardetzky,[3] and Robert A. Lamb[1,2]*

Howard Hughes Medical Institute[1] and Department of Biochemistry, Molecular Biology, and Cell Biology,[2] Northwestern University, Evanston, Illinois 60208-3500, and Department of Structural Biology, Stanford University School of Medicine, Stanford, California 94305[3]

Received 10 June 2009/Accepted 14 August 2009

For paramyxoviruses, entry requires a receptor-binding protein (hemagglutinin-neuraminidase [HN], H, or G) and a fusion protein (F). Like other class I viral fusion proteins, F is expressed as a prefusion metastable protein that undergoes a refolding event to induce fusion. HN binding to its receptor triggers F refolding by an unknown mechanism. HN may serve as a clamp that stabilizes F in its prefusion state until HN binds the target cell (the "clamp model"). Alternatively, HN itself may undergo a conformational change after receptor binding that destabilizes F and causes F to trigger (the "provocateur model"). To examine F-HN interactions by bimolecular fluorescence complementation (BiFC), the cytoplasmic tails of parainfluenza virus 5 (PIV5) F and HN were fused to complementary fragments of yellow fluorescent protein (YFP). Coexpression of the BiFC constructs resulted in fluorescence; however, coexpression with unrelated BiFC constructs also produced fluorescence. The affinity of the two halves of YFP presumably superseded the F-HN interaction. Unexpectedly, coexpression of the BiFC F and HN constructs greatly enhanced fusion in multiple cell types. We hypothesize that the increase in fusion occurs because the BiFC tags bring F and HN together more frequently than occurs in a wild-type (wt) scenario. This implies that normally much of wt F is not associated with wt HN, in conflict with the clamp model for activation. Correspondingly, we show that wt PIV5 fusion occurs in an HN concentration-dependent manner. Also inconsistent with the clamp model are the findings that BiFC F does not adopt a postfusion conformation when expressed in the absence of HN and that HN coexpression does not provide resistance to the heat-induced triggering of F. In support of a provocateur model of F activation, we demonstrate by analysis of the morphology of soluble F trimers that the hyperfusogenic mutation S443P has a destabilizing effect on F.

Most enveloped viruses use a single protein to bind to their cellular receptor, and this protein also mediates fusion with a target membrane (19, 68). In contrast, paramyxoviruses use different glycoproteins for these two functions, with receptor binding mediated by a protein variously called hemagglutinin-neuraminidase (HN), H, or G, depending on the virus, and with viral fusion mediated by a metastable F protein that undergoes a refolding event to induce fusion (28, 54). The mechanism by which the receptor-binding protein communicates with the fusion protein is not well understood. The general requirement of a homotypic attachment protein indicates that HN, H, and G function in fusion in more than their receptor-binding capacities and that the receptor-binding protein must interact specifically with F (6, 9, 21, 24, 39).

The structures of multiple receptor-binding proteins have been resolved, and the similarity among the structures suggests that they may trigger fusion though a common mechanism (7, 11, 14, 20, 30, 70, 75). The parainfluenza virus 5 (PIV5) HN structure revealed a tetramer comprising a pair of dimers and only very minor conformational differences between the native and receptor-bound states (75). Similarly, the structures of Nipah virus (NiV) G in its native and receptor-bound states did not reveal a major conformational change (7, 70). These observations led to the proposal that a tetrameric rearrangement of HN, H, or G after receptor binding may be the signal that triggers the fusion protein (29, 75). Newcastle disease virus (NDV) HN crystallizes in two dimeric orientations, one with minimal dimer interactions and the other with an extensive dimer interface (14); however, it is unlikely that a transition between these forms triggers fusion because the addition of a disulfide bond that precludes the formation of the minimal-interface dimeric form does not prevent fusion activation (35). The stalk was not resolved in any of the attachment protein crystal structures; however, the HN stalk appears to be tetrameric, flexible, and predominantly helical (74). Multiple studies using chimeric HN or H molecules have mapped the F-interacting region to the stalk of the attachment protein (6, 15, 16, 31, 59, 65, 66). In addition, mutations in the stalks of HN, H, and G have been shown to inhibit fusion activation (4, 13, 37, 38, 49, 58). Interpretation of the findings from mutational studies is complicated by the fact that these proteins are multifunctional and any mutation may alter simultaneously attachment, fusion promotion, and in the case of HN, neuraminidase (NA) activity. Monoclonal antibodies (MAbs) that bind the attachment protein and neutralize infection without blocking receptor binding have been mapped to the stalk of

* Corresponding author. Mailing address: BMBCB, Northwestern University, 2205 Tech Drive, Hogan 2-100, Evanston, IL 60208-3500. Phone: (847) 491-5433. Fax: (847) 491-2467. E-mail: ralamb@northwestern.edu.

† Supplemental material for this article may be found at http://jvi.asm.org/.

▽ Published ahead of print on 26 August 2009.

PIV2 HN (76) and the base of the head of NiV G (1). Furthermore, a change in NiV G conformation upon receptor binding was detected using circular dichroism and was attributed to the stalk region (1).

Paramyxovirus F is a class I fusion protein, and the structures of prefusion PIV5 F (73) and postfusion NDV and human PIV3 F proteins have been solved (10, 72). F is expressed as a trimer that is proteolytically cleaved to liberate the N terminus of the fusion peptide. After triggering, helical region A (HRA) adjacent to the fusion peptide undergoes a major conformational change that extends the fusion peptide outward for insertion into the target membrane. This process forms a prehairpin intermediate that is anchored in two membranes. Helical region B (HRB) adjacent to the transmembrane domain then translocates to bind to HRA, forming a six-helix bundle and the postfusion hairpin conformation. The binding of exogenous peptides to the refolding intermediate forms of F indicates that the HRB stalk region opens before HRA extends. In the absence of HN, the open-stalk intermediate requires a temperature of 37°C to form; however, this intermediate can form at 4°C when HN is coexpressed, suggesting that HN can influence the conformation of the prefusion HRB stalk (52). Studies of chimeric F molecules have implicated residues in both the head and stalk of F in the interaction with HN or H (31, 64).

Two models have emerged to describe the triggering mechanism for fusion and the way in which F is regulated to refold at the right time and place. In the "clamp model," the attachment protein acts to retain the F protein in its prefusion metastable form. In this model, HN and F are associated on the cell surface and when HN binds the receptor, F is released and triggered to refold to drive membrane merging. In the "provocateur model," the attachment protein actively triggers the metastable F by destabilizing it. After receptor binding, HN undergoes a conformational change that destabilizes F. In this model, HN may be preassociated with F, or HN may be induced to associate with F after receptor binding. A major difference between these models is that in the clamp model, HN exerts a stabilizing effect on prefusion F whereas in the provocateur model, HN exerts a destabilizing effect on prefusion F.

Studies examining the triggering of paramyxoviruses have focused on the coimmunoprecipitation (coIP) of F and its receptor-binding partner, HN, H, or G. For measles virus (MeV), NiV, and Hendra virus (HeV), analyses of mutants have shown an inverse correlation between fusion promotion and the strength of F-H or F-G interaction (2, 5, 48). These results have been interpreted to support the clamp model of activation, although the correlation of high affinity with low fusogenicity does not demonstrate causation. In contrast, mutations that decrease the fusion of NDV correlate with decreased F-HN interaction (38). It has been suggested previously that paramyxoviruses that use proteinaceous receptors (via H or G) may have a different triggering mechanism from those that use sialic acid as a receptor (via HN) (25), despite the close structural homology of HN, H, and G.

Detecting a complex of PIV5 F and HN by biochemical methods has been difficult. To examine the association of F and HN during fusion, we employed yellow fluorescent protein (YFP) in bimolecular fluorescence complementation (BiFC) by linking the N-terminal region of YFP (Yn) to one protein and the C-terminal region of YFP (Yc) to a second protein. If the two proteins associate, the two YFP segments are brought together to form a complete YFP that fluoresces. BiFC permits the detection of transient or low-affinity interactions in intact cells by monitoring a gain in fluorescence (27). The technique has been used successfully to study the interactions of herpesvirus glycoproteins (3), another set of interacting glycoproteins for which coIP has proven difficult. Our results show that enhancing the F-HN interaction promotes fusion and that HN exerts a destabilizing effect on F, in support of the provocateur model of fusion activation over the clamp model.

MATERIALS AND METHODS

Cells, antibodies, and constructs. Vero cells were maintained in Dulbecco's modified Eagle's medium (DMEM) supplemented with 10% fetal calf serum (FCS). BHK-21 cells were supplemented with 10% tryptose phosphate broth. BSR-T7 cells (BHK cells expressing T7 polymerase) were grown in DMEM–10% FCS with 1 mg/ml G418 added on every third passage (8). HeLa-CD4-LTR-β-gal cells (AIDS Research and Reference Reagent Program) were used for their high transfection efficiency and were grown in the presence of 200 μg/ml G418, 100 μg/ml hygromycin, and 20 mM HEPES, pH 7.4. Sf9 cells were grown in Sf-900 medium supplemented with 10% FCS. High Five cells were grown in Express Five medium with 18 mM GlutaMax medium (Invitrogen, Carlsbad, CA).

Antibodies specific for F included MAb F1a ascites fluid (50); MAb 6-7 hybridoma supernatant, an antibody raised against the equivalent to the hyperfusogenic PIV5 S443P mutant F (63); polyclonal antibody (PAb) vacF, a rabbit serum raised against F expressed by vaccinia virus (44); and PAb anti-F2 peptide, a rabbit serum raised against a mixture of peptides from F2 (22). Antibodies specific for HN included MAb HN-1b and HN-5a ascites fluids and MAb HN-4b hybridoma supernatant (50); PAb SDS-HN serum, raised against denatured HN; and PAb R9721 serum, raised against the purified HN ectodomain expressed by baculovirus (75).

The BiFC F and HN constructs were cloned into pCAGGS by four-primer PCR. The Yn fragment (residues 1 to 174) and the Yc fragment (residues 174 to 239) of Venus YFP (41, 56) were derived from pBR771 and pBR772 templates (3) and added to the cytoplasmic tails of F and HN via a diglycine linker. The native HN start codon was removed and a new start codon was added for Yc-HN.

Flow cytometry. To quantify cell surface expression and determine F protein conformation, HeLa-CD4-LTR-β-gal cells were transfected overnight with plasmids encoding the F or HN constructs by using Lipofectamine Plus (Invitrogen). Cells were stained with undiluted MAb 6-7 or a 1:100 dilution of MAb F1a, PAb vacF, or PAb R9721, followed by a fluorescein isothiocyanate-labeled secondary antibody diluted 1:100. Prior to the addition of MAb 6-7, warmed phosphate-buffered saline (PBS) was added to the cells and the plates were incubated at 37, 42, 50, or 60°C for 10 min and then washed with cold PBS. The fluorescence intensity of 10,000 cells was measured by using a FACSCalibur flow cytometer (Becton Dickinson, Franklin Lakes, NJ).

Cell-based enzyme-linked immunosorbent assay (ELISA). To confirm cell surface expression, Vero cells were transfected overnight with plasmids encoding the HN constructs as described above. Cells were replated at confluence onto 96-well plates, incubated overnight, and stained with serial dilutions of PAb R9721. Cells were washed, fixed in 4% paraformaldehyde, and incubated with a horseradish peroxidase-conjugated secondary antibody at 1:1,000. After being washed, cells were rinsed with 20 mM citrate buffer, pH 4.5, ABTS [2,2′-azino-bis(3-ethylbenzthiazolinesulfonic acid)] peroxidase substrate (Moss, Inc., Pasadena, MD) was added, and the absorbance at 405 nm was detected with a SpectraMax M5 plate reader (Molecular Devices, Sunnyvale, CA).

Hemadsorption (HAd) assay. HeLa-CD4-LTR-β-gal cells in 12-well plates were transfected in triplicate overnight with plasmids encoding the HN constructs by using Lipofectamine Plus (Invitrogen). The cells were rinsed, and 300 μl/well of 1% human red blood cells (RBCs) in DMEM containing 50 mM HEPES, pH 7.4, was added for 1 h at 4°C on a rocker. Cells were washed three times with cold DMEM and twice with cold PBS supplemented with 2 mM (each) $CaCl_2$ and $MgCl_2$. RBCs were lysed in 250 μl/well lysis buffer (145 mM NH_4Cl, 17 mM Tris-HCl, pH 7.4) for 10 min at room temperature on a rocker. Supernatants (200 μl/sample) were transferred into 96-well plates, and absorbance at 410 nm was measured.

NA assay. HeLa-CD4-LTR-β-gal cells in six-well plates were transfected in triplicate overnight with plasmids encoding the HN constructs by using Lipofectamine Plus (Invitrogen). Cells were released using 500 μl/well 530 μM EDTA in PBS. Cells were resuspended in 1 ml of PBS supplemented with 2 mM (each) $CaCl_2$ and $MgCl_2$ and pelleted for 5 min at 800 rpm and 4°C. The cell pellets were resuspended in 100 μl of 125 mM sodium acetate buffer (pH 4.75) containing 6.25 mM $CaCl_2$, and then 25 μl of 5 mM 4-methylumbelliferyl-*N*-acetyl-α-D-neuraminic acid (Sigma-Aldrich, St. Louis, MO) was added. Reaction mixtures were incubated at 37°C with occasional mixing. After 30 min, 75 μl of 20 mM sodium carbonate buffer (pH 10.4) was added. Cells were pelleted at 14,000 rpm, and supernatants (180 μl/sample) were transferred into a 96-well plate. Fluorescence was measured using excitation and emission wavelengths of 356 and 450 nm, respectively.

Fluorescence microscopy. HeLa-CD4-LTR-β-gal cells on coverslips were transfected overnight as described above. When indicated, cells were treated overnight with 100 mU/ml NA from *Clostridium perfringens* (Sigma, St. Louis, MO), starting at 5 h posttransfection. Nonpermeabilized cells were fixed in 4% formaldehyde in PBS, mounted in Prolong Gold (Invitrogen), and visualized using an LSM5 Pascal confocal microscope (Zeiss, Thornswood, NY) with a 63× objective. For immunofluorescence, cells were stained for 1 h with MAb 6-7 at 1:10 or MAb F1a at 1:100, followed by an Alexa-594-conjugated secondary antibody at 1:200 for 1 h.

Fusion assays. For the syncytium formation assay, cells were transfected with plasmids encoding the various F and HN constructs as described above. Cells were incubated overnight and stained using Hema 3 (Fisher Healthcare, Houston, TX). For the initial luciferase assays, confluent Vero cells in six-well plates were transfected using 4 μl of Lipofectamine, 4 μl of Plus reagent, and 800 ng/well each of pCAGGS-F, pCAGGS-HN, and pT7-luc, a plasmid encoding luciferase under the control of the T7 promoter. After overnight incubation, cells were overlaid with BSR-T7 cells and incubated for 8 h. Cells were lysed in 300 μl/well reporter lysis buffer (Promega, Madison, WI) and frozen overnight. To read luciferase activity, 150 μl of a luciferase assay substrate (Promega) was added to 200 μl of lysate and relative light units (RLU) were determined using a SpectraMax M5 plate reader (Molecular Devices). For the luciferase assays examining HN titration, DNA levels used in transfection were adjusted as described in the legend to Fig. 6.

Radioimmunoprecipitation. To quantitate expression levels in the luciferase assay, Vero cells were transfected as described above or infected with PIV5 strain W3A at 3 PFU/cell overnight. Cells were starved for 30 min in methionine- and cysteine-free DMEM and radiolabeled with a 1-h pulse of 100 μCi/well ^{35}S-Promix followed by a 1.5-h chase. Cell surface proteins were biotinylated by two 10-min incubations on ice with 1.5 mg/ml EZ-Link sulfo-*N*-hydroxysuccinimide-biotin (Pierce, Rockford, IL) in PBS, pH 8. The reaction was quenched by three washes in 50 mM glycine, and cells were lysed in ice-cold RIPA buffer (1% sodium deoxycholate, 1% Triton X-100, 0.1% SDS, 10 mM Tris-Cl, pH 7.4) containing 150 mM NaCl and protease inhibitors. The lysates were subjected to ultracentrifugation for 10 min at 100,000 × *g*, and antibodies (20 μl of anti-F2 peptide or 10 μl of HN-1b, 10 μl of HN-5a, and 20 μl of HN-4b) were added. After 2 h at 4°C, immune complexes were adsorbed onto 30 μl of protein A Sepharose for 1 h at 4°C. Samples were washed twice with RIPA buffer containing 300 mM NaCl, twice with RIPA buffer containing 150 mM NaCl, and once with 50 mM Tris buffer containing 150 mM NaCl and 2.5 mM EDTA. Samples were resuspended in 50 μl/tube 50 mM Tris containing 0.5% SDS and boiled for 5 min. Supernatants were diluted in a 1-ml solution of 20 mM Tris, pH 8.0, containing 150 mM NaCl, 5 mM EDTA, 1% Triton X-100, and 0.2% bovine serum albumin, and 50 μl/tube streptavidin-agarose was added. After overnight incubation at 4°C, samples were washed again as described above and boiled in dithiothreitol (DTT)-containing loading buffer. Proteins were analyzed by SDS-polyacrylamide gel electrophoresis (PAGE) on 10% acrylamide gels and visualized using an FLA-5100 phosphorimager (Fujifilm, Stamford, CT). To examine the coIP of F-Yn and Yc-HN, cells were transfected as described above, except without the luciferase-encoding plasmid, and processed as described above.

To assess endoglycosidase H sensitivity, HeLa-CD4-LTR-β-gal cells were transfected overnight and radiolabeled with 150 μCi/well by a 15-min pulse. After the chase times indicated below, total cell lysates were clarified as described above. Antibodies (20 μl of anti-F2 peptide or 20 μl of PAb SDS-HN) were added, and samples were immunoprecipitated and washed as described above. Samples were resuspended in 50 mM Tris containing 0.5% SDS (45 μl/tube) and boiled. Following the addition of a 45-μl/tube solution of 100 mM sodium citrate, pH 5.5, containing 2 mM phenylmethylsulfonyl fluoride, supernatants were divided into duplicate samples and 5 mU of endoglycosidase H (Roche, Germany) was added to half of the samples. Samples were incubated overnight at 37°C, and proteins were analyzed by SDS-PAGE as described above.

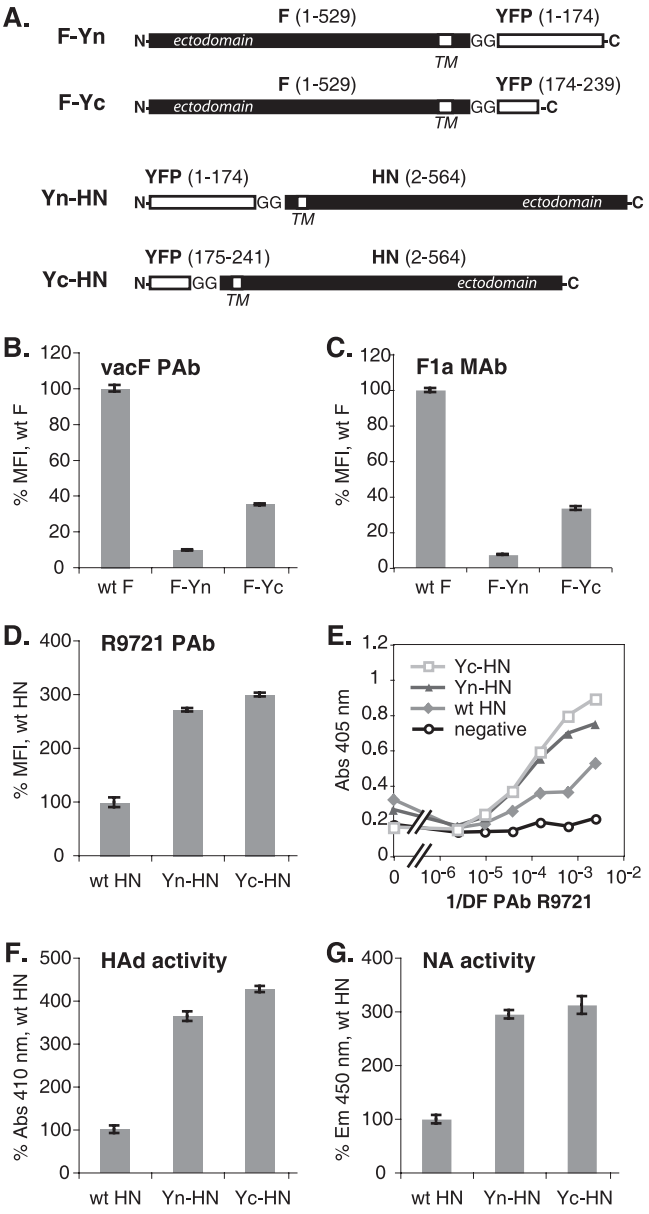

FIG. 1. Expression of BiFC constructs. (A) Schematic diagram of F and HN BiFC constructs. The N- and C-terminal halves of YFP were added to the cytoplasmic tails of W3A F and HN via a diglycine linker. TM, transmembrane domain. (B to D) Levels of surface expression of the F and HN constructs on transfected HeLa-CD4-LTR-β-gal cells were determined by flow cytometry using the anti-F PAb vacF, the anti-F MAb F1a, or the anti-HN PAb R9721. The mean fluorescence intensity (MFI) is shown as a percentage of wt protein levels. (E) Levels of surface expression of the HN constructs on transfected Vero cells were determined by cell-based ELISA using the PAb R9721. Abs, absorbance; 1/DF, reciprocal of dilution factor. (F) The HAd activities of the HN constructs were determined by measuring RBC binding to transfected HeLa-CD4-LTR-β-gal cells by spectroscopy. (G) The NA activities of the HN constructs on transfected HeLa-CD4-LTR-β-gal cells were determined using a fluorimetric assay. Em, emission.

For clarity, the F-containing samples were boiled in a nonreducing loading buffer that lacked DTT to allow F1 and F2 to remain disulfide linked.

To examine protein stability, HeLa-CD4-LTR-β-gal cells were transfected overnight and radiolabeled with a 30-min pulse of 70 μCi/well. After a chase of 1 to 3 h, cell lysates were clarified and immunoprecipitated as described above,

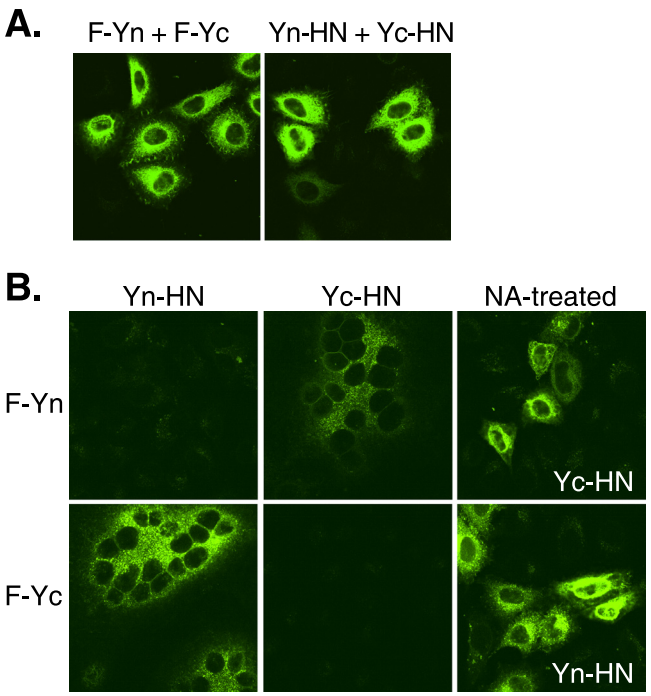

FIG. 2. BiFC analyses. Transfected HeLa-CD4-LTR-β-gal cells expressing the F and HN constructs were fixed at 20 h posttransfection and examined for YFP fluorescence. (A) BiFC analyses of F or HN oligomers. (B) BiFC analyses of F and HN complexes. NA-treated samples were incubated with NA starting at 4 h posttransfection.

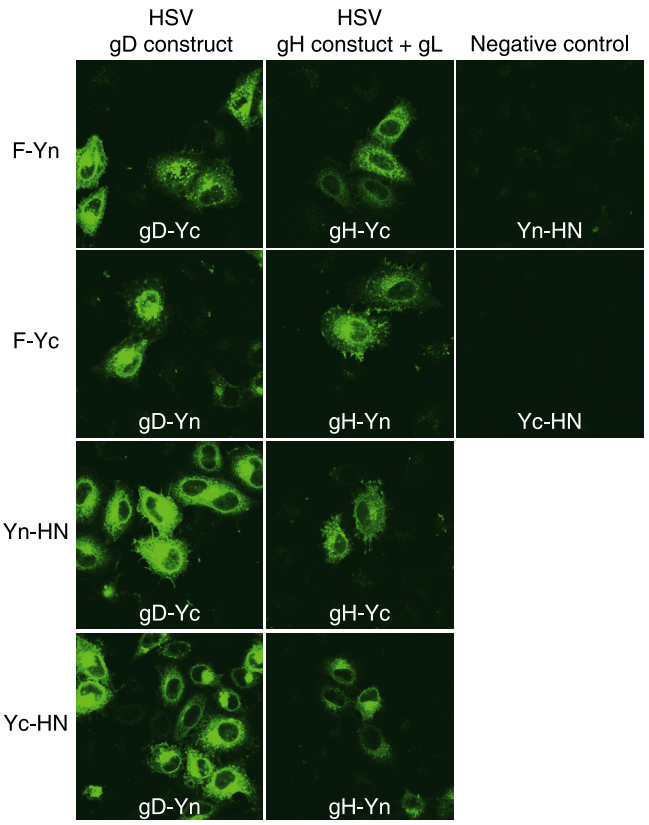

FIG. 3. BiFC with heterologous glycoproteins. Transfected HeLa-CD4-LTR-β-gal cells expressing combinations of PIV5 or HSV glycoprotein constructs were fixed at 20 h posttransfection and examined for YFP fluorescence. For the negative controls, cells were transfected with pairs of noncomplementary YFP halves.

using anti-F2 peptide or HN-1b, HN-5a, and HN-4b. Samples were washed, boiled in DTT-containing loading buffer, and analyzed by SDS-PAGE.

To assess the furin cleavage of F, HeLa-CD4-LTR-β-gal cells were transfected and radiolabeled as described above. After chase times of up to 5 h, surface proteins were biotinylated as described above. F was immunoprecipitated as described above, and samples were boiled in 90 μl/tube 50 mM Tris containing 0.5% SDS. Supernatants were divided into duplicate samples, and half of the samples were incubated with streptavidin-agarose and treated as described above.

Baculovirus generation and expression. The purified soluble protein F-GCNt used in this work is similar to the previously published F-GCNt (73), except for the omission of a factor Xa site prior to the His tag and the use of a different signal sequence. cDNA encoding the ectodomain of PIV5 F (from the W3A strain) was cloned into the pBACgus vector (Novagen, Madison, WI) by PCR. The signal sequence was replaced with that of baculovirus gp64, the F_0 precursor furin cleavage site was mutated to prevent intracellular processing, the transmembrane domain was replaced with a trimerization domain (GCNt) in heptad repeat phase with HRB, and a six-His tag was added to the C terminus. Mutations encoding P22L or S443P were added to the plasmid using the QuikChange kit (Stratagene, La Jolla, CA). Recombinant baculoviruses were generated using the BacVector 3000 transfection kit (Novagen) and plaque purified on Sf9 cells. F-GCNt was expressed and purified essentially as described previously (73). High Five cells were grown in suspension and infected with recombinant baculovirus. Cell supernatants were harvested, dialyzed, and incubated with nickel-nitrilotriacetic acid resin (Qiagen, Valencia, CA). Proteins were eluted from the resin using increasing concentrations of imidazole buffer (10 to 250 mM) in 50 mM Tris–150 mM NaCl, pH 8.

EM. Electron microscopy (EM) was performed as described previously (69). Samples were absorbed onto freshly prepared thin carbon film supported on 300-mesh copper grids that were glow discharged prior to use, and stained with 0.1% uranyl formate. Grids were examined with a JEOL 1230 transmission electron microscope operating at 100 kV. The electron microscope was capable of resolving the lattice plane spacing of catalase crystals (6.85 and 8.75 nm).

RESULTS

Cell surface expression of BiFC constructs is altered. To examine PIV5 F and HN interactions by BiFC, the cytoplasmic tails of each protein were fused to complementary fragments of YFP (3, 56). The N-terminal (Yn) or C-terminal (Yc) portion of YFP was added to the F and HN tails via a diglycine linker (Fig. 1A). The cell surface expression of these proteins was examined by flow cytometry. The F-Yn and F-Yc constructs were expressed on the cell surface, but at a reduced level compared to wild-type (wt) F, as judged by immunoreactivity with both the prefusion conformation-specific MAb F1a (12) and the PAb vacF (Fig. 1B and C). Coexpression with a complementary HN BiFC construct did not enhance the surface expression of the F BiFC constructs significantly (data not shown). Yn-HN and Yc-HN surface expression was increased compared to that of wt HN (Fig. 1D). The expression of the HN proteins was confirmed also by using cell-based ELISA because wt HN introduced by transfection yields low fluorescence intensity as measured by flow cytometry (Fig. 1E). In accordance with the elevated levels of surface expression, cells transfected with the BiFC HN constructs exhibited enhanced HAd and NA activities compared to cells transfected with wt HN (Fig. 1F and G).

All of the BiFC constructs exhibited delayed acquisition of endoglycosidase H resistance compared to the wt (see Fig. S1

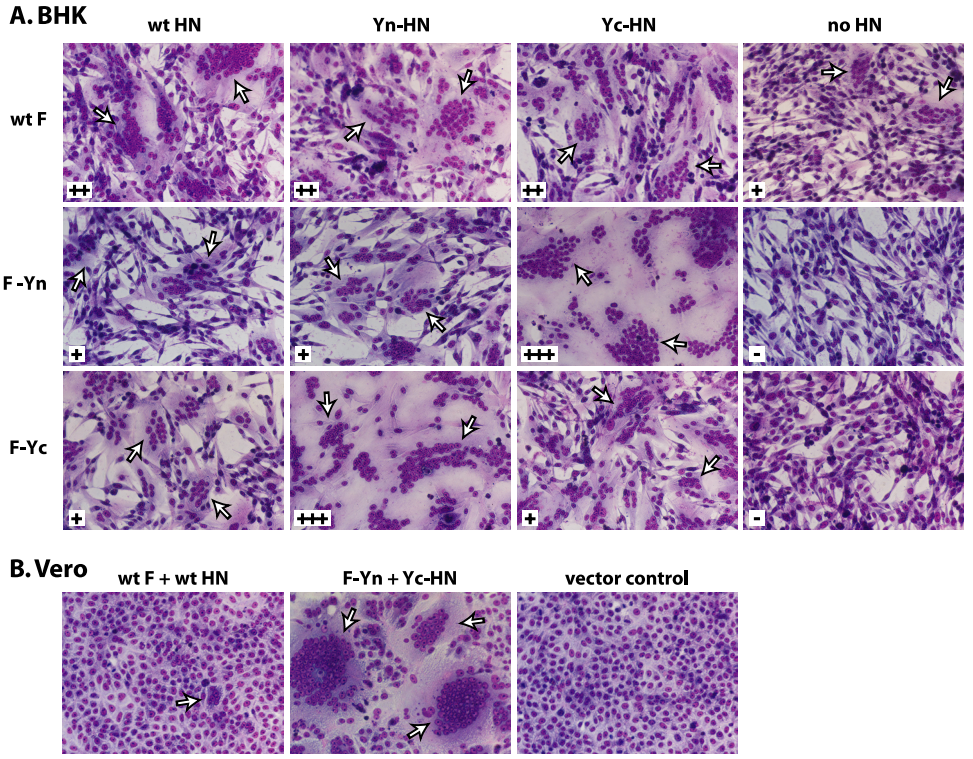

FIG. 4. BiFC constructs mediate enhanced syncytium formation. BHK or Vero cells were transfected with plasmids encoding the F and HN constructs, and the cells were imaged 24 h posttransfection. Syncytium formation is graded as follows from least to most: −, +, ++, and +++. Arrows indicate syncytia.

in the supplemental material); however, the BiFC constructs were not more rapidly degraded than wt F and HN (see Fig. S2A in the supplemental material). Although a minor, fast-migrating band of Yc-HN was seen, it did not accumulate over time. Furin cleavage of F-Yn and F-Yc was reduced, with the cleaved F-Yn preferentially reaching the cell surface (see Fig. S2 in the supplemental material). Thus, the BiFC modifications of the cytoplasmic tails of F and HN altered expression, resulting in decreased levels of F and increased levels of HN on the cell surface.

Coexpression of the F and HN BiFC constructs results in fluorescence. To test the abilities of the BiFC constructs to complement one another, cells were cotransfected with the constructs. Oligomers of F-Yn–F-Yc or Yn-HN–Yc-HN yielded fluorescence with a pattern indicating intracellular and cell surface localization (Fig. 2A). When cells were cotransfected with F and HN BiFC constructs carrying complementary YFP fragments, fluorescence was observed at the cell surface and within the cells (Fig. 2B). Fluorescence occurred both after fusion and when fusion was prevented by the addition of NA to destroy the receptor for HN. No fluorescence was observed when the BiFC constructs were expressed individually or together with a noncomplementary BiFC partner.

Coexpression of unrelated BiFC constructs also produces fluorescence. The cotransfection of cells with the F and HN BiFC constructs and herpes simplex virus (HSV) glycoprotein BiFC constructs (3) also resulted in complementation. The Yn- and Yc-containing F and HN constructs each interacted with HSV gB, gD, or a gH-gL complex (Fig. 3 and data not shown). This result was not anticipated and suggested that the affinity of the two halves of YFP superseded the F-HN interaction. Transfecting the cells with smaller amounts of plasmid to reduce expression levels did not eliminate the complementation between unrelated constructs (data not shown). We attempted to demonstrate the specificity of the F-HN interaction by adjusting the amount of the wt F plasmid in the transfection mixture to displace F-Yn from an F-Yn–Yc-HN complex, but the inclusion of up to 1.8 μg of wt F plasmid in the transfection mixture did not disrupt the fluorescence produced by 75 ng each of F-Yn and Yc-HN plasmids (data not shown).

Coexpression of F and HN BiFC constructs enhances fusion. Unexpectedly, the coexpression of the BiFC F and HN constructs in multiple cell types, including BHK-21, Vero, and HeLa-CD4-LTR-β-gal cells, was observed to enhance syncytium formation (Fig. 4 and data not shown). PIV5 F can mediate the fusion of BHK-21 cells in the absence of HN expression, but the coexpression of HN enhances fusion (Fig. 4) (53). F-Yn and F-Yc did not mediate fusion in the absence of HN, most likely due to low cell surface expression levels. The coexpression of a complementary BiFC HN construct and F-Yn or F-Yc increased fusion to levels even higher than that seen with wt F and HN. On Vero and HeLa-CD4-LTR-β-gal cells, wt F and HN produce only small and rare syncytia, but the coexpression of complementary F and HN BiFC constructs resulted in remarkable syncytium formation. While F-HN complementation increased levels of fusion, fusion did not become receptor independent. The removal of sialic acid by NA still prevented cell-cell fusion (Fig. 2B).

The fusion mediated by the BiFC constructs was quantitated using a luciferase assay. When cells were cotransfected with

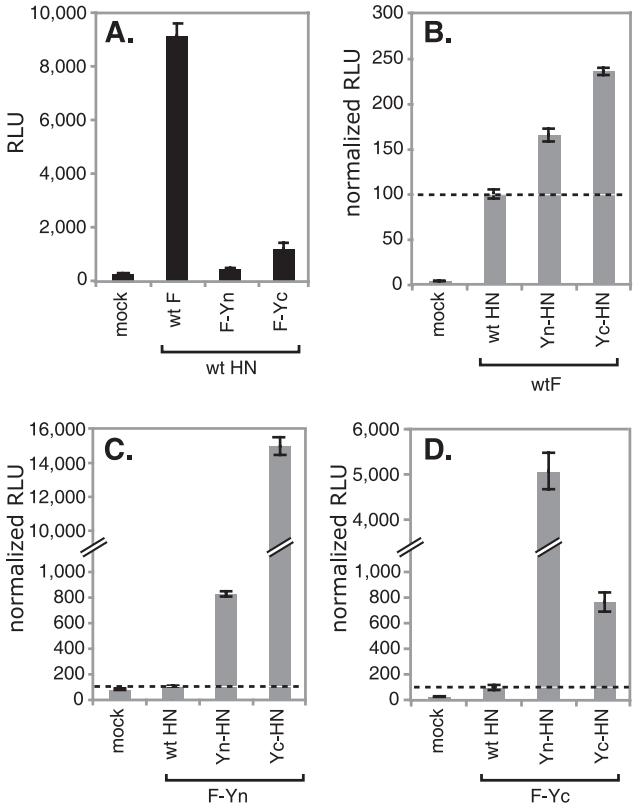

FIG. 5. BiFC constructs mediate enhanced fusion. Vero cells were transfected with plasmids encoding F, HN, and luciferase under the control of the T7 polymerase promoter. Cells were overlaid with BSR-T7 cells at 20 h posttransfection. After 7 h, the cells were lysed and the luciferase activity (expressed in RLU) was determined. (A) Comparison of the degrees of fusion mediated by wt F, F-Yn, and F-Yc when the proteins are coexpressed with wt HN. (B to D) Degrees of fusion mediated by wt F (B), F-Yn (C), and F-Yc (D) when the proteins are coexpressed with wt HN, Yn-HN, or Yc-HN. For each F construct, the data were normalized by setting the RLU obtained after coexpression with wt HN at 100%. All samples were analyzed in parallel, and the standard deviations of results for triplicate samples are shown.

the F constructs and wt HN, the levels of fusion mediated by the F constructs correlated directly with the levels of surface expression of the F proteins (Fig. 5A). Adding Yn or Yc to the tail of F did not alter its fusogenicity inherently. When wt F and the BiFC HN constructs were coexpressed, fusion mediated by wt F was enhanced somewhat, most likely due to the higher levels of surface expression of these HN proteins (Fig. 5B). When F-Yn was expressed with its complementary partner Yc-HN, fusion was increased by 150-fold over the level obtained by coexpression with wt HN (Fig. 5C). Similarly, when F-Yc was expressed with Yn-HN, fusion was enhanced 50-fold (Fig. 5D). The coexpression of noncomplementary Yn-HN and F-Yn (Fig. 5C) or Yc-HN and F-Yc (Fig. 5D) resulted in a more moderate enhancement in fusion, most likely due to the enhanced levels of surface expression of Yn-HN and Yc-HN.

Fusion is HN-concentration dependent. We hypothesize that the observed increase in fusion occurred because the BiFC tags bring F and HN together more frequently or for a longer duration than occurs with wt F and HN expression. If this is true, then increasing the level of HN on the cell surface should enhance F occupancy (HN association with F) and increase fusion. Correspondingly, we have shown that wt PIV5 fusion occurs in an HN concentration-dependent manner (Fig. 6A). Fusion mediated by F-Yn also is dependent on the concentration of Yc-HN (Fig. 6B). As expected, transfecting cells with more HN plasmid resulted in higher levels of HN surface expression (Fig. 6C). The expression levels of F and HN in these experiments were similar to those achieved during virus infection. At high levels of HN expression, fusion begins to plateau, presumably because the majority of the F trimers available for fusion are occupied by association with HN. Although the fusion mediated by wt F and HN and that mediated by the BiFC constructs begin to plateau at similar levels of HN expression, the F-Yn- and Yc-HN-mediated fusion reaches a much greater maximum level, consistent with the higher levels of fusion observed previously (Fig. 4 and 5).

Previously, PIV5 fusion was shown not to be dependent on HN concentration (17); however, that work was performed with different cells and a transfection protocol that required vaccinia virus infection for expression. The present transfection protocol may have increased sensitivity for detecting the effects of PIV5 HN expression levels on fusion, possibly due to lessened cell cytotoxicity in the absence of vaccinia virus infection.

When Yc-HN was immunoprecipitated from cells, a slower-migrating band coprecipitated (Fig. 6C). Further analysis demonstrated that this band is the same size as F_0-Yn (see Fig. S3 in the supplemental material). The coIP of F-Yn but not wt F with Yc-HN is consistent with the BiFC tags increasing the F-HN interaction.

HN coexpression does not alter the heat-induced triggering of F. If the BiFC tags enhance fusion by bringing F and HN together more frequently, this situation implies that normally much of wt F is unoccupied by association with HN, a conclusion in conflict with the clamp model for activation. In the provocateur model, unoccupied F can wait at the surface in a prefusion conformation for HN to bind the receptor and interact with F to trigger fusion. In the clamp model, F expressed in the absence of HN would be less able to retain a prefusion conformation.

The conformation of F on the cell surface can be examined using the postfusion conformation-specific MAb 6-7 (12, 63) and the prefusion conformation-specific MAb F1a (12, 50). F can be triggered to convert to its postfusion conformation by using heat as a surrogate triggering mechanism (12). If HN was a clamp for F, it might be expected to provide resistance to the heat-induced triggering of F. Thus, transfected HeLa-CD4-LTR-β-gal cells expressing F and/or HN were heated for 10 min at temperatures up to 60°C and analyzed by flow cytometry using MAbs 6-7 and F1a. When F was expressed alone, it showed greatly increased reactivity to MAb 6-7 at elevated temperatures and a corresponding loss in reactivity to MAb F1a (Fig. 7A and B). HN coexpression did not alter the heat-induced MAb 6-7 reactivity (Fig. 7B). In fact, after treatment at 60°C, MAb 6-7 reactivity may be enhanced slightly with HN coexpression, possibly indicating that expression with HN causes F to be more easily triggered by heat. To demonstrate that 60°C does not denature the F protein, the morphology of

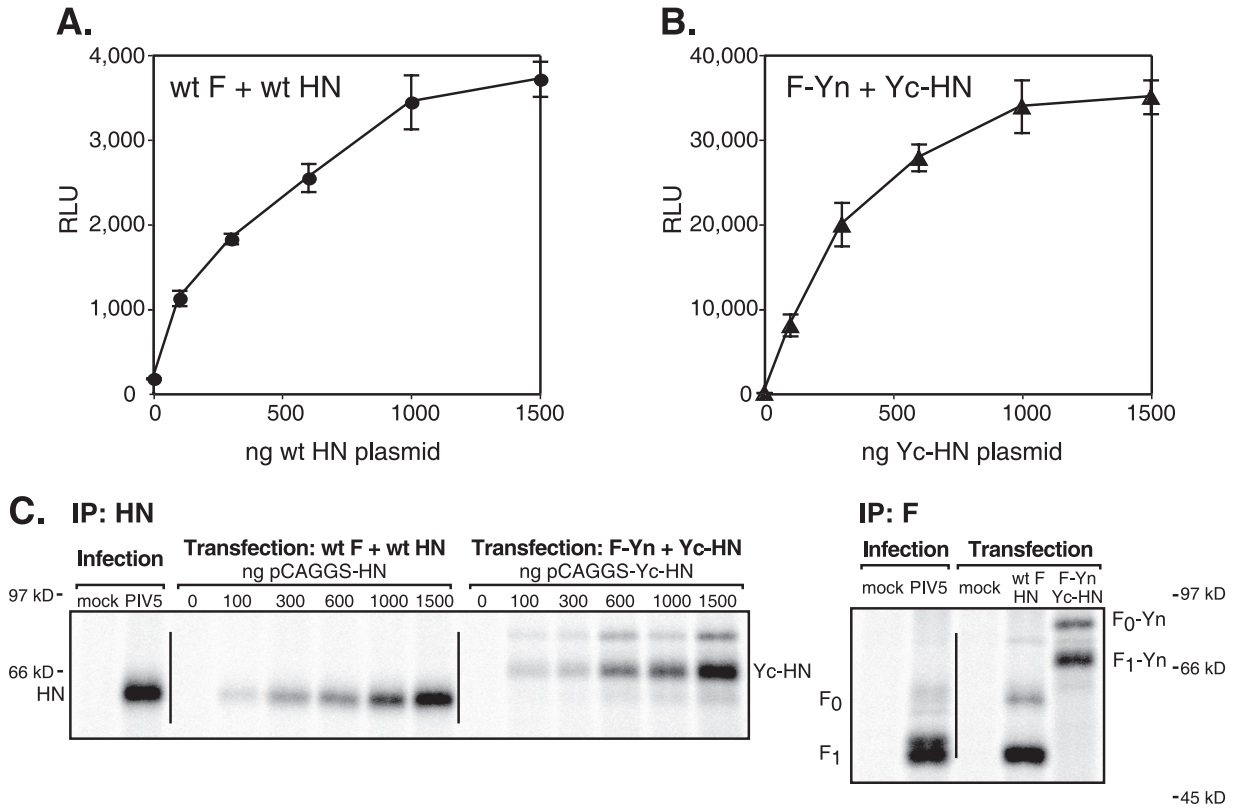

FIG. 6. F-mediated fusion is dependent on the HN concentration. (A and B) Vero cells were transfected with plasmids encoding luciferase (400 ng/well) and wt F or F-Yn (400 ng/well) and increasing amounts of plasmid encoding HN or Yc-HN. Cells were overlaid with BSR-T7 cells at 20 h posttransfection. After 7 h, the cells were lysed and the luciferase activity (expressed in RLU) was determined. The standard deviations of results for triplicate samples are shown. (C) Vero cells were transfected as described in the legend to panels A and B or infected with PIV5 at 3 PFU/cell for comparison. Cells were radiolabeled, surface proteins were biotinylated, and surface-expressed F or HN was immunoprecipitated (IP) and visualized by SDS-PAGE. For the anti-F IP, the amount of HN or Yc-HN DNA used in cotransfection was 1,500 ng/well.

purified soluble F (F-GCNt) after heating was examined by EM (Fig. 7C). As anticipated, the "ball-and-stem" morphology of the prefusion trimers was converted to a "golf tee" postfusion morphology after heating (12), but the protein did not unfold or aggregate.

The conversion of F-Yn to a postfusion conformation depends on Yc-HN coexpression and fusion. In contrast to the HeLa-CD4-LTR-β-gal cells cotransfected with plasmids expressing wt F and HN, cells cotransfected with the BiFC constructs form large syncytia that are too fragile to be analyzed by flow cytometry. Thus, the conformation of the BiFC F constructs was analyzed by immunofluorescence microscopy. When F-Yn and Yc-HN were coexpressed in HeLa-CD4-LTR-β-gal cells, MAb 6-7 reactivity was detected on the syncytia, indicating the presence of the postfusion form of F (Fig. 8). When cells were treated with exogenous NA, fluorescence complementation was detected but fusion was blocked and MAb 6-7 reactivity was not induced. Notably, F-Yn expressed alone was positive for MAb F1a reactivity but negative for MAb 6-7 reactivity. This finding indicates that in the absence of HN, F-Yn was not expressed in a postfusion conformation, in contrast to the predictions of the clamp model. This experiment was also performed using cells transfected with plasmids expressing wt F and wt HN (data not shown); however, no gain in MAb 6-7 reactivity after incubation at 37°C was observed, most likely because fusion was much less extensive and fewer wt F trimers were triggered.

The hyperfusogenic mutation S443P is destabilizing. The two models of activation have different implications for the effect of HN on the stability of F; HN stabilizes F in the clamp model and destabilizes F in the provocateur model. PIV5 F can mediate HN-independent fusion at a low level (Fig. 4) (23). If HN was required to clamp F in its prefusion conformation, this HN-independent fusion would have to be explained by the action of a subpopulation of F proteins able to retain a prefusion conformation without HN. A destabilizing mutation in F would diminish this surviving prefusion population and thus reduce fusion.

To further investigate the mechanism of prefusion F triggering, we analyzed the effects of known hypofusogenic or hyperfusogenic mutations on the stability of prefusion F (26, 45). We expressed and purified soluble F proteins (F-GCNt) carrying a hypofusogenic P22L or a hyperfusogenic S443P mutation and visualized the F-GCNt trimer morphology by EM (12). F-GCNt and P22L mutant F-GCNt adopted a prefusion conformation resembling a ball and stem (Fig. 9A and B), whereas the S443P mutant F-GCNt protein adopted a postfusion conformation resembling a golf tee (Fig. 9C). Thus, as anticipated (45), the hyperfusogenic S443P mutation destabilizes the F-GCNt protein. If HN enhanced fusion by stabilizing F, as

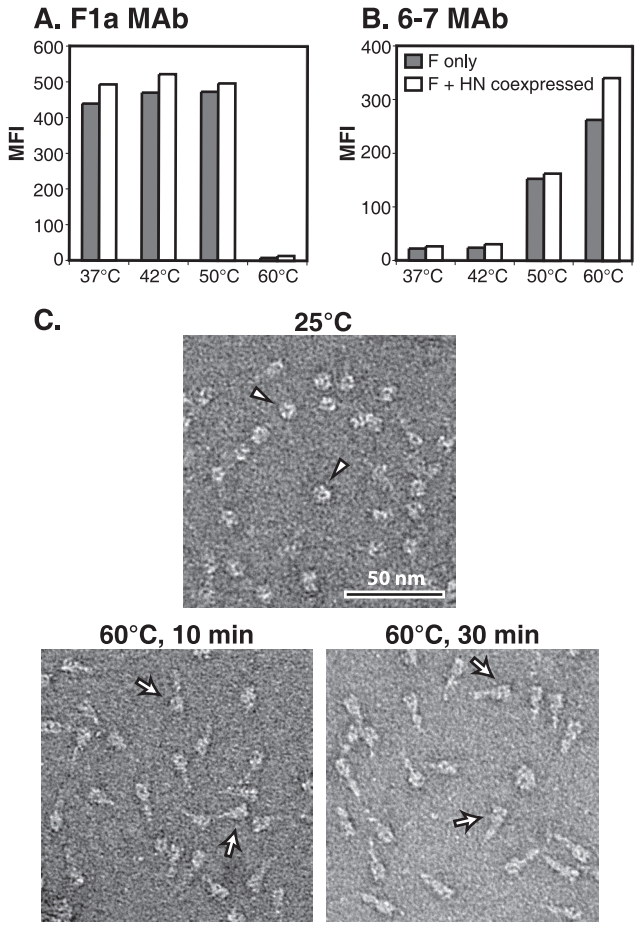

FIG. 7. HN coexpression does not alter the heat-induced triggering of F. (A and B) Transfected HeLa-CD4-LTR-β-gal cells expressing F only (gray bars) or both F and HN (white bars) were heated to the indicated temperatures for 10 min at 24 h posttransfection. Cell surface reactivity with MAb 6-7 or MAb F1a was analyzed by flow cytometry. MFI, mean fluorescence intensity. (C) A soluble form of PIV5 F (F-GCNt) was expressed in insect cells by a recombinant baculovirus, and secreted F protein was purified. Trimers were visualized by EM before or after being heated to 60°C for 10 or 30 min.

proposed in the clamp model, the destabilizing mutation S443P should have increased HN dependence. On the contrary, S443P mutant F mediates fusion better than wt F in the absence of HN (26, 45, 53). The fact that this destabilizing S443P mutation enhances fusion in both the presence and absence of HN is consistent with the provocateur model and argues against the clamp model. In accordance with an anticipated stabilizing effect (26, 45), the hypofusogenic P22L mutation did not convert F-GCNt into a postfusion conformation. As with wt F, when Yn was added to full-length F carrying P22L, complementation with Yc-HN facilitated more fusion than wt HN (Fig. 9D).

DISCUSSION

Paramyxoviruses employ two separate proteins to achieve receptor binding and fusion, but how the attachment protein physically communicates with the fusion protein to mediate membrane merging at the appropriate time and place is unclear. Receptor binding presumably triggers a conformational change in the attachment protein that transmits a signal to F. Two conflicting models of fusion activation exist. In the clamp model, F and an attachment protein associate intracellularly and this association stabilizes the prefusion conformation of F. Upon receptor binding, the attachment protein disengages from F, allowing F to trigger. In the provocateur model, binding to the receptor elicits an interaction between F and an attachment protein on the cell surface that destabilizes F and thereby triggers it. Although the provocateur model does not necessitate intracellular association, it is not precluded.

Other class I fusion machines, such as human immunodeficiency virus gp41, are proposed to be activated by disengagement of the receptor-binding subunit (68); however, unlike paramyxovirus F, gp41 is expressed with its receptor-binding subunit gp120 as a single protein that is processed. When the gp41 subunit is expressed alone, the protein adopts a postfusion conformation (67). Although HN is always coexpressed with F during virus infection, the requirement of HN for F function is not absolute because cells transfected with PIV5 F alone can form syncytia (23, 42). Similarly, respiratory syncytial virus and metapneumovirus F proteins can mediate fusion in the absence of an attachment protein (55, 61).

The interaction between F and its attachment protein has been examined biochemically, and although the coIP of PIV5 F and HN has been difficult, coIP has been demonstrated for multiple paramyxoviruses including PIV2, NDV, MeV, NiV, HeV, and respiratory syncytial virus (5, 15, 18, 32, 34, 47, 57, 71). Results from studies comparing the effects of mutations on coIP efficiency versus fusion promotion provide support for both models of fusion activation. In support of the clamp model, an inverse correlation between F-H or F-G affinity and fusion promotion has been shown for MeV, NiV, and HeV (1, 2, 5, 13, 46, 48). In contrast, a direct correlation between F-HN affinity and fusion promotion has been shown for NDV (15, 37, 38), in support of the provocateur model. Since fusion-deficient MeV H stalk mutants show enhanced coIP with F (13) and fusion-deficient NDV HN stalk mutants show decreased coIP with F (38), it has been proposed that viruses with proteinaceous receptors may employ a different mechanism of fusion activation from those using the sialic acid receptor (25). Regardless, these correlations prove neither model definitively, and interpretation of the results is confounded by the fact that some observations do not fit into this breakdown easily. A mutation in the active site of NDV HN can block fusion without preventing F-HN association (33), some HeV G stalk mutants with decreased fusion lose F association (4), and some MeV F transmembrane mutants with enhanced fusion show improved F1-H association (40). In addition, NA treatment of cells to remove the receptor resulted in enhanced NDV F-HN coIP, consistent with the clamp model (36). The clamp model obligates the intracellular association of F and its attachment protein. Unfortunately, analyses of the intracellular association of F and H or HN by an endoplasmic reticulum coretention approach have yielded conflicting results (43, 47, 60, 62).

To examine the mechanism of PIV5 fusion activation in an intact cell without relying on coIP, we linked complementary fragments of YFP to the cytoplasmic tails of F and HN and examined the F-HN interaction by using BiFC. Unexpectedly,

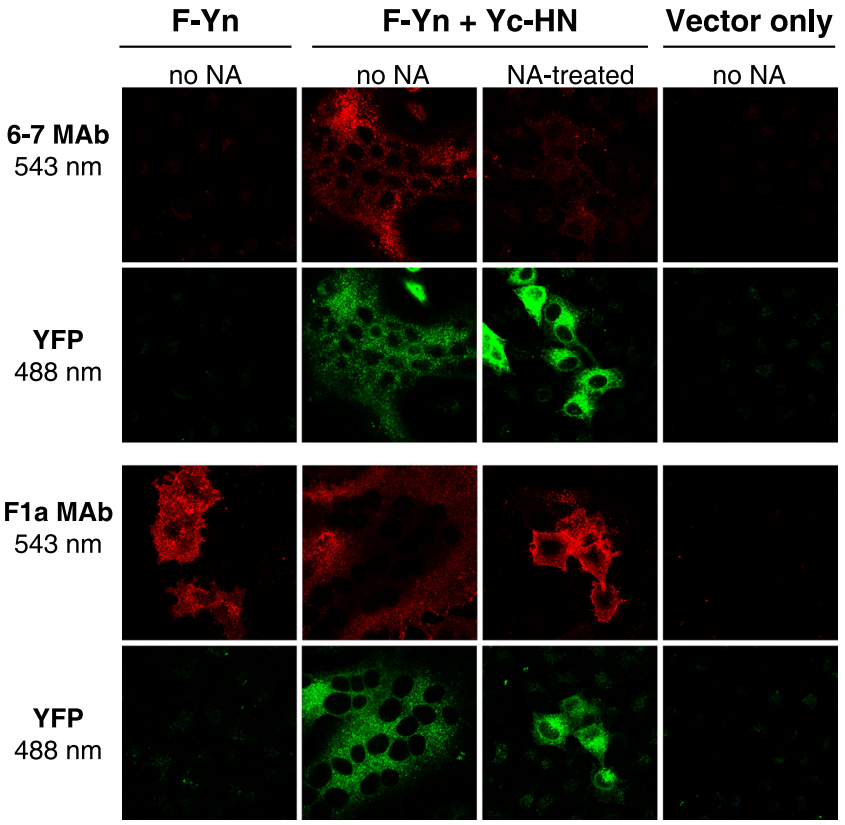

FIG. 8. BiFC constructs trigger postfusion-specific MAb 6-7 reactivity after fusion. HeLa-CD4-LTR-β-gal cells were transfected with F-Yn and Yc-HN constructs and incubated overnight in the presence or absence of NA to block syncytium formation. Cells were stained with MAb 6-7 or F1a and imaged by confocal microscopy.

adding the BiFC tags enhanced F-HN association (see Fig. S3 in the supplemental material). The binding of the YFP fragments to each other may have been aided by the fact that F and HN are both oligomeric and anchored in a membrane that restricts diffusion within a bidimensional space. Although we were unable to monitor F-HN association during fusion because the affinity of the YFP fragments superseded the F-HN interaction (Fig. 3), adding complementary BiFC tags to the tails of F and HN vastly enhanced cell-cell fusion (Fig. 4 and 5). Unlike other mutants that exhibit enhanced fusion, the BiFC constructs possess wt sequences for the entirety of F and HN, excluding the addition to the cytoplasmic tails. The hyperfusogenic phenotype cannot be attributed to mutations that alter the inherent stability of F because the phenotype is seen only when the expressed F and HN BiFC constructs are complementary. We propose that the fusion is enhanced because BiFC brings F and HN together more frequently or for a longer duration than occurs normally. Correspondingly, increasing HN expression levels was shown to enhance PIV5 fusion (Fig. 6).

If PIV5 fusion was activated as described in the clamp model, HN would exert a stabilizing force on F. In contrast, the coexpression of HN did not provide resistance to the heat-induced triggering of F (Fig. 7). In addition, F expressed in the absence of HN did not spontaneously adopt the postfusion conformation (Fig. 8). If the provocateur model of PIV5 fusion activation is correct, HN exerts a destabilizing force on F. Whereas F did not adopt a postfusion conformation when expressed alone, F did convert to its postfusion form after the coexpression of HN and syncytium formation (Fig. 8). In addition, elevating temperature can enhance fusion mediated by F expressed in the absence of HN (45). The fact that a destabilizing force such as heat can be used as a surrogate for HN suggests that HN also supplies a destabilizing effect.

We previously suggested that the hyperfusogenic mutation S443P has a destabilizing effect on the F protein (45). EM analysis of purified soluble F protein carrying this mutation confirmed that S443P is destabilizing because the mutant is expressed in its postfusion conformation (Fig. 9). Thus, a destabilizing mutation in F enhances fusion. The destabilizing S443P mutation does not elevate the HN dependence of F, as may be expected if HN was required as a clamp. In fact, the opposite is observed; S443P mutant F mediates more extensive HN-independent fusion than wt F. Accordingly, the hypofusogenic mutation P22L is not destabilizing. These findings are consistent with the immunoreactivities of the S443P and P22L mutants with the postfusion conformation-specific MAb 6-7. S443P mutant F displays enhanced MAb 6-7 reactivity, and P22L mutant F displays reduced MAb 6-7 reactivity (51).

The findings from our investigation of the energetics of the F-HN interaction support the provocateur model of fusion activation, a model that is consistent with the coIP results for NDV F-HN complexes (25). It remains to be seen whether the mechanism of fusion activation differs for other paramyxovi-

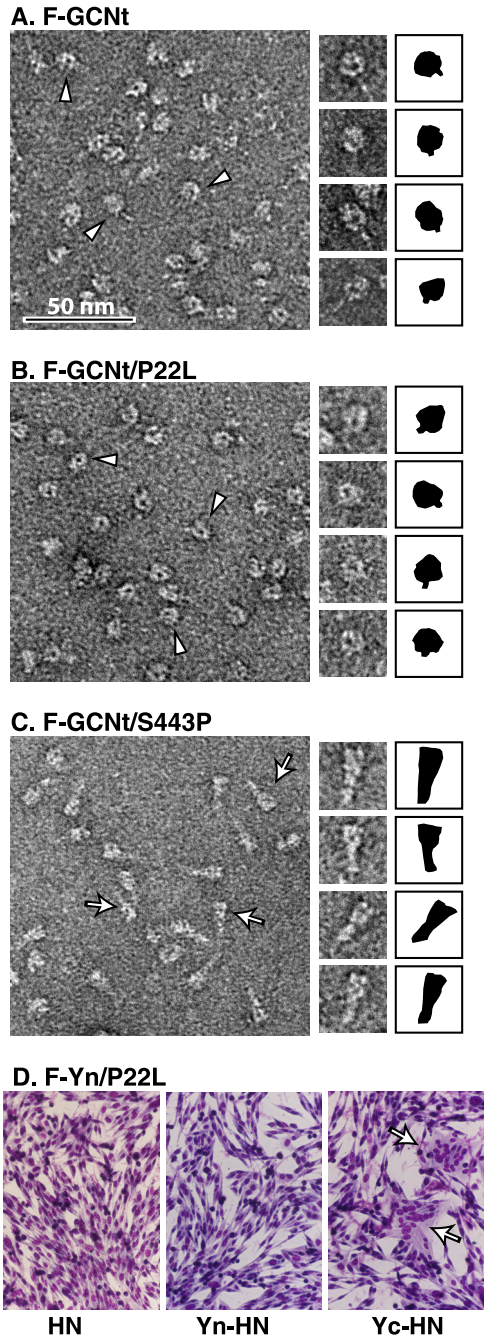

FIG. 9. P22L is a stabilizing mutation, and S443P is a destabilizing mutation. (A to C) Wild-type (A), P22L mutant (B), or S443P mutant (C) soluble forms of PIV5 F (F-GCNt) were expressed and purified using baculovirus. Trimers were visualized by EM, and those with prefusion (arrowheads) or postfusion (arrows) morphology are noted. The shapes of individual trimers are depicted in black to the right of the images. (D) BHK cells were transfected with plasmids encoding the F-Yn P22L mutant and wt HN, Yn-HN, or Yc-HN. Cells were imaged 24 h posttransfection.

ruses. The difficulty in immunoprecipitating a PIV5 F-HN complex implies that the interaction has low affinity or is transient. The dynamics and kinetics of the F-HN association, as well as the specific conformational changes that occur in HN after receptor binding and subsequently in F, remain to be determined.

ACKNOWLEDGMENTS

We thank Gary Cohen, Roselyn Eisenberg, and J. Charles Whitbeck for the herpesvirus BiFC constructs and advice. The JEOL 1230 electron microscope used in this study is part of the Biological Imaging Facility at Northwestern University.

S.A.C. is an associate and R.A.L. is an investigator of the Howard Hughes Medical Institute. This research was supported in part by grant R01 AI-23173 from the National Institute of Allergy and Infectious Diseases, National Institutes of Health.

REFERENCES

1. **Aguilar, H. C., Z. A. Ataman, V. Aspericueta, A. Q. Fang, M. Stroud, O. A. Negrete, R. A. Kammerer, and B. Lee.** 2009. A novel receptor-induced activation site in the Nipah virus attachment glycoprotein (G) involved in triggering the fusion glycoprotein (F). J. Biol. Chem. **284:**1628–1635.
2. **Aguilar, H. C., K. A. Matreyek, C. M. Filone, S. T. Hashimi, E. L. Levroney, O. A. Negrete, A. Betrolotti-Ciarlet, D. Y. Choi, I. McHardy, J. A. Fulcher, S. V. Su, M. C. Wolf, L. Kohatsu, L. G. Baum, and B. Lee.** 2006. N-glycans on Nipah virus fusion protein protect against neutralization but reduce membrane fusion and viral entry. J. Virol. **80:**4878–4889.
3. **Atanasiu, D., J. C. Whitbeck, T. M. Cairns, B. Reilly, G. H. Cohen, and R. J. Eisenberg.** 2007. Bimolecular complementation reveals that glycoproteins gB and gH/gL of herpes simplex virus interact with each other during cell fusion. Proc. Natl. Acad. Sci. USA **104:**18718–18723.
4. **Bishop, K. A., A. C. Hickey, D. Khetawat, J. R. Patch, K. N. Bossart, Z. Zhu, L. F. Wang, D. S. Dimitrov, and C. C. Broder.** 2008. Residues in the stalk domain of the Hendra virus G glycoprotein modulate conformational changes associated with receptor binding. J. Virol. **82:**11398–11409.
5. **Bishop, K. A., T. S. Stantchev, A. C. Hickey, D. Khetawat, K. N. Bossart, V. Krasnoperov, P. Gill, Y. R. Feng, L. Wang, B. T. Eaton, L. F. Wang, and C. C. Broder.** 2007. Identification of Hendra virus G glycoprotein residues that are critical for receptor binding. J. Virol. **81:**5893–5901.
6. **Bousse, T., T. Takimoto, W. L. Gorman, T. Takahashi, and A. Portner.** 1994. Regions on the hemagglutinin-neuraminidase proteins of human parainfluenza virus type-1 and Sendai virus important for membrane fusion. Virology **204:**506–514.
7. **Bowden, T. A., M. Crispin, D. J. Harvey, A. R. Aricescu, J. M. Grimes, E. Y. Jones, and D. I. Stuart.** 2008. Crystal structure and carbohydrate analysis of Nipah virus attachment glycoprotein: a template for antiviral and vaccine design. J. Virol. **82:**11628–11636.
8. **Buchholz, U. J., S. Finke, and K. K. Conzelmann.** 1999. Generation of bovine respiratory syncytial virus (BRSV) from cDNA: BRSV NS2 is not essential for virus replication in tissue culture, and the human RSV leader region acts as a functional BRSV genome promoter. J. Virol. **73:**251–259.
9. **Cattaneo, R., and J. K. Rose.** 1993. Cell fusion by the envelope glycoproteins of persistent measles viruses which cause lethal human brain disease. J. Virol. **67:**1493–1502.
10. **Chen, L., J. J. Gorman, J. McKimm-Breschkin, L. J. Lawrence, P. A. Tulloch, B. J. Smith, P. M. Colman, and M. C. Lawrence.** 2001. The structure of the fusion glycoprotein of Newcastle disease virus suggests a novel paradigm for the molecular mechanism of membrane fusion. Structure **9:**255–266.
11. **Colf, L. A., Z. S. Juo, and K. C. Garcia.** 2007. Structure of the measles virus hemagglutinin. Nat. Struct. Mol. Biol. **14:**1227–1228.
12. **Connolly, S. A., G. P. Leser, H. S. Yin, T. S. Jardetzky, and R. A. Lamb.** 2006. Refolding of a paramyxovirus F protein from prefusion to postfusion conformations observed by liposome binding and electron microscopy. Proc. Natl. Acad. Sci. USA **103:**17903–17908.
13. **Corey, E. A., and R. M. Iorio.** 2007. Mutations in the stalk of the measles virus hemagglutinin protein decrease fusion but do not interfere with virus-specific interaction with the homologous fusion protein. J. Virol. **81:**9900–9910.
14. **Crennell, S., T. Takimoto, A. Portner, and G. Taylor.** 2000. Crystal structure of the multifunctional paramyxovirus hemagglutinin-neuraminidase. Nat. Struct. Biol. **7:**1068–1074.
15. **Deng, R., Z. Wang, P. J. Mahon, M. Marinello, A. Mirza, and R. M. Iorio.** 1999. Mutations in the Newcastle disease virus hemagglutinin-neuraminidase protein that interfere with its ability to interact with the homologous F protein in the promotion of fusion. Virology **253:**43–54.
16. **Deng, R., Z. Wang, A. M. Mirza, and R. M. Iorio.** 1995. Localization of a domain on the paramyxovirus attachment protein required for the promotion of cellular fusion by its homologous fusion protein spike. Virology **209:**457–469.
17. **Dutch, R. E., S. B. Joshi, and R. A. Lamb.** 1998. Membrane fusion promoted by increasing surface densities of the paramyxovirus F and HN proteins: comparison of fusion reactions mediated by simian virus 5 F, human parainfluenza virus type 3 F, and influenza virus HA. J. Virol. **72:**7745–7753.

18. **Feldman, S. A., R. L. Crim, S. A. Audet, and J. A. Beeler.** 2001. Human respiratory syncytial virus surface glycoproteins F, G and SH form an oligomeric complex. Arch. Virol. **146:**2369–2383.
19. **Harrison, S. C.** 2008. Viral membrane fusion. Nat. Struct. Mol. Biol. **15:**690–698.
20. **Hashiguchi, T., M. Kajikawa, N. Maita, M. Takeda, K. Kuroki, K. Sasaki, D. Kohda, Y. Yanagi, and K. Maenaka.** 2007. Crystal structure of measles virus hemagglutinin provides insight into effective vaccines. Proc. Natl. Acad. Sci. USA **104:**19535–19540.
21. **Heminway, B. R., Y. Yu, and M. S. Galinski.** 1994. Paramyxovirus mediated cell fusion requires co-expression of both the fusion and hemagglutinin-neuraminidase glycoproteins. Virus Res. **31:**1–16.
22. **Horvath, C. M., and R. A. Lamb.** 1992. Studies on the fusion peptide of a paramyxovirus fusion glycoprotein: roles of conserved residues in cell fusion. J. Virol. **66:**2443–2455.
23. **Horvath, C. M., R. G. Paterson, M. A. Shaughnessy, R. Wood, and R. A. Lamb.** 1992. Biological activity of paramyxovirus fusion proteins: factors influencing formation of syncytia. J. Virol. **66:**4564–4569.
24. **Hu, X., R. Ray, and R. W. Compans.** 1992. Functional interactions between the fusion protein and hemagglutinin-neuraminidase of human parainfluenza viruses. J. Virol. **66:**1528–1534.
25. **Iorio, R. M., and P. J. Mahon.** 2008. Paramyxoviruses: different receptors—different mechanisms of fusion. Trends Microbiol. **16:**135–137.
26. **Ito, M., M. Nishio, M. Kawano, S. Kusagawa, H. Komada, Y. Ito, and M. Tsurudome.** 1997. Role of a single amino acid at the amino terminus of the simian virus 5 F2 subunit in syncytium formation. J. Virol. **71:**9855–9858.
27. **Kerppola, T. K.** 2006. Design and implementation of bimolecular fluorescence complementation (BiFC) assays for the visualization of protein interactions in living cells. Nat. Protoc. **1:**1278–1286.
28. **Lamb, R. A., and T. S. Jardetzky.** 2007. Structural basis of viral invasion: lessons from paramyxovirus F. Curr. Opin. Struct. Biol. **17:**427–436.
29. **Lamb, R. A., R. G. Paterson, and T. S. Jardetzky.** 2006. Paramyxovirus membrane fusion: lessons from the F and HN atomic structures. Virology **344:**30–37.
30. **Lawrence, M. C., N. A. Borg, V. A. Streltsov, P. A. Pilling, V. C. Epa, J. N. Varghese, J. L. McKimm-Breschkin, and P. M. Colman.** 2004. Structure of the haemagglutinin-neuraminidase from human parainfluenza virus type III. J. Mol. Biol. **335:**1343–1357.
31. **Lee, J. K., A. Prussia, T. Paal, L. K. White, J. P. Snyder, and R. K. Plemper.** 2008. Functional interaction between paramyxovirus fusion and attachment proteins. J. Biol. Chem. **283:**16561–16572.
32. **Levroney, E. L., H. C. Aguilar, J. A. Fulcher, L. Kohatsu, K. E. Pace, M. Pang, K. B. Gurney, L. G. Baum, and B. Lee.** 2005. Novel innate immune functions for galectin-1: galectin-1 inhibits cell fusion by Nipah virus envelope glycoproteins and augments dendritic cell secretion of proinflammatory cytokines. J. Immunol. **175:**413–420.
33. **Li, J., E. Quinlan, A. Mirza, and R. M. Iorio.** 2004. Mutated form of the Newcastle disease virus hemagglutinin-neuraminidase interacts with the homologous fusion protein despite deficiencies in both receptor recognition and fusion promotion. J. Virol. **78:**5299–5310.
34. **Low, K. W., T. Tan, K. Ng, B. H. Tan, and R. J. Sugrue.** 2008. The RSV F and G glycoproteins interact to form a complex on the surface of infected cells. Biochem. Biophys. Res. Commun. **366:**308–313.
35. **Mahon, P. J., A. M. Mirza, T. A. Musich, and R. M. Iorio.** 2008. Engineered intermonomeric disulfide bonds in the globular domain of Newcastle disease virus hemagglutinin-neuraminidase protein: implications for the mechanism of fusion promotion. J. Virol. **82:**10386–10396.
36. **McGinnes, L. W., and T. G. Morrison.** 2006. Inhibition of receptor binding stabilizes Newcastle disease virus HN and F protein-containing complexes. J. Virol. **80:**2894–2903.
37. **Melanson, V. R., and R. M. Iorio.** 2006. Addition of N-glycans in the stalk of the Newcastle disease virus HN protein blocks its interaction with the F protein and prevents fusion. J. Virol. **80:**623–633.
38. **Melanson, V. R., and R. M. Iorio.** 2004. Amino acid substitutions in the F-specific domain in the stalk of the Newcastle disease virus HN protein modulate fusion and interfere with its interaction with the F protein. J. Virol. **78:**13053–13061.
39. **Morrison, T., C. McQuain, and L. McGinnes.** 1991. Complementation between avirulent Newcastle disease virus and a fusion protein gene expressed from a retrovirus vector: requirements for membrane fusion. J. Virol. **65:** 813–822.
40. **Muhlebach, M. D., V. H. Leonard, and R. Cattaneo.** 2008. The measles virus fusion protein transmembrane region modulates availability of an active glycoprotein complex and fusion efficiency. J. Virol. **82:**11437–11445.
41. **Nagai, T., K. Ibata, E. S. Park, M. Kubota, K. Mikoshiba, and A. Miyawaki.** 2002. A variant of yellow fluorescent protein with fast and efficient maturation for cell-biological applications. Nat. Biotechnol. **20:**87–90.
42. **Paterson, R. G., S. W. Hiebert, and R. A. Lamb.** 1985. Expression at the cell surface of biologically active fusion and hemagglutinin-neuraminidase proteins of the paramyxovirus simian virus 5 from cloned cDNA. Proc. Natl. Acad. Sci. USA **82:**7520–7524.
43. **Paterson, R. G., M. L. Johnson, and R. A. Lamb.** 1997. Paramyxovirus fusion (F) protein and hemagglutinin-neuraminidase (HN) protein interactions: intracellular retention of F and HN does not affect transport of the homotypic HN or F protein. Virology **237:**1–9.
44. **Paterson, R. G., R. A. Lamb, B. Moss, and B. R. Murphy.** 1987. Comparison of the relative roles of the F and HN surface glycoproteins of the paramyxovirus simian virus 5 in inducing protective immunity. J. Virol. **61:**1972–1977.
45. **Paterson, R. G., C. J. Russell, and R. A. Lamb.** 2000. Fusion protein of the paramyxovirus SV5: destabilizing and stabilizing mutants of fusion activation. Virology **270:**17–30.
46. **Plemper, R. K., and R. W. Compans.** 2003. Mutations in the putative HR-C region of the measles virus F_2 glycoprotein modulate syncytium formation. J. Virol. **77:**4181–4190.
47. **Plemper, R. K., A. L. Hammond, and R. Cattaneo.** 2001. Measles virus envelope glycoproteins hetero-oligomerize in the endoplasmic reticulum. J. Biol. Chem. **276:**44239–44246.
48. **Plemper, R. K., A. L. Hammond, D. Gerlier, A. K. Fielding, and R. Cattaneo.** 2002. Strength of envelope protein interaction modulates cytopathicity of measles virus. J. Virol. **76:**5051–5061.
49. **Porotto, M., M. Murrell, O. Greengard, and A. Moscona.** 2003. Triggering of human parainfluenza virus 3 fusion protein (F) by the hemagglutinin-neuraminidase (HN) protein: an HN mutation diminishes the rate of F activation and fusion. J. Virol. **77:**3647–3654.
50. **Randall, R. E., D. F. Young, K. K. A. Goswami, and W. C. Russell.** 1987. Isolation and characterization of monoclonal antibodies to simian virus 5 and their use in revealing antigenic differences between human, canine and simian isolates. J. Gen. Virol. **68:**2769–2780.
51. **Russell, C. J., T. S. Jardetzky, and R. A. Lamb.** 2004. Conserved glycine residues in the fusion peptide of the paramyxovirus fusion protein regulate activation of the native state. J. Virol. **78:**13727–13742.
52. **Russell, C. J., T. S. Jardetzky, and R. A. Lamb.** 2001. Membrane fusion machines of paramyxoviruses: capture of intermediates of fusion. EMBO J. **20:**4024–4034.
53. **Russell, C. J., K. L. Kantor, T. S. Jardetzky, and R. A. Lamb.** 2003. A dual-functional paramyxovirus F protein regulatory switch segment: activation and membrane fusion. J. Cell Biol. **163:**363–374.
54. **Russell, C. J., and L. E. Luque.** 2006. The structural basis of paramyxovirus invasion. Trends Microbiol. **14:**243–246.
55. **Schowalter, R. M., S. E. Smith, and R. E. Dutch.** 2006. Characterization of human metapneumovirus F protein-promoted membrane fusion: critical roles for proteolytic processing and low pH. J. Virol. **80:**10931–10941.
56. **Shyu, Y. J., H. Liu, X. Deng, and C. D. Hu.** 2006. Identification of new fluorescent protein fragments for bimolecular fluorescence complementation analysis under physiological conditions. BioTechniques **40:**61–66.
57. **Stone-Hulslander, J., and T. G. Morrison.** 1997. Detection of an interaction between the HN and F proteins in Newcastle disease virus-infected cells. J. Virol. **71:**6287–6295.
58. **Stone-Hulslander, J., and T. G. Morrison.** 1999. Mutational analysis of heptad repeats in the membrane-proximal region of Newcastle disease virus HN protein. J. Virol. **73:**3630–3637.
59. **Tanabayashi, K., and R. W. Compans.** 1996. Functional interaction of paramyxovirus glycoproteins: identification of a domain in Sendai virus HN which promotes cell fusion. J. Virol. **70:**6112–6118.
60. **Tanaka, Y., B. R. Heminway, and M. S. Galinski.** 1996. Down-regulation of paramyxovirus hemagglutinin-neuraminidase glycoprotein surface expression by a mutant fusion protein containing a retention signal for the endoplasmic reticulum. J. Virol. **70:**5005–5015.
61. **Techaarpornkul, S., N. Barretto, and M. E. Peeples.** 2001. Functional analysis of recombinant respiratory syncytial virus deletion mutants lacking the small hydrophobic and/or attachment glycoprotein gene. J. Virol. **75:**6825–6834.
62. **Tong, S., and R. W. Compans.** 1999. Alternative mechanisms of interaction between homotypic and heterotypic parainfluenza virus HN and F proteins. J. Gen. Virol. **80:**107–115.
63. **Tsurudome, M., M. Ito, M. Nishio, M. Kawano, H. Komada, and Y. Ito.** 2001. Hemagglutinin-neuraminidase-independent fusion activity of simian virus 5 fusion (F) protein: difference in conformation between fusogenic and nonfusogenic F proteins on the cell surface. J. Virol. **75:**8999–9009.
64. **Tsurudome, M., M. Ito, M. Nishio, M. Kawano, K. Okamoto, S. Kusagawa, H. Komada, and Y. Ito.** 1998. Identification of regions on the fusion protein of human parainfluenza virus type 2 which are required for haemagglutinin-neuraminidase proteins to promote cell fusion. J. Gen. Virol. **79:**279–289.
65. **Tsurudome, M., M. Kawano, T. Yuasa, N. Tabata, M. Nishimo, H. Komada, and Y. Ito.** 1995. Identification of regions on the hemagglutinin-neuraminidase protein of human parainfluenza virus type 2 important for promoting cell fusion. Virology **213:**190–203.
66. **Wang, Z., A. M. Mirza, J. Li, P. J. Mahon, and R. M. Iorio.** 2004. An oligosaccharide at the C-terminus of the F-specific domain in the stalk of the human parainfluenza virus 3 hemagglutinin-neuraminidase modulates fusion. Virus Res. **99:**177–185.
67. **Weissenhorn, W., S. A. Wharton, L. J. Calder, P. L. Earl, B. Moss, E. Aliprandis, J. J. Skehel, and D. C. Wiley.** 1996. The ectodomain of HIV-1 env subunit

gp41 forms a soluble, alpha-helical, rod-like oligomer in the absence of gp120 and the N-terminal fusion peptide. EMBO J. **15:**1507–1514.

68. **White, J. M., S. E. Delos, M. Brecher, and K. Schornberg.** 2008. Structures and mechanisms of viral membrane fusion proteins: multiple variations on a common theme. Crit. Rev. Biochem. Mol. Biol. **43:**189–219.
69. **Wrigley, N. G., E. Brown, and R. K. Chillingworth.** 1982. Combining accurate defocus with low-dose imaging in high resolution electron microscopy of biological material. J. Microsc. **130:**225–232.
70. **Xu, K., K. R. Rajashankar, Y. P. Chan, J. P. Himanen, C. C. Broder, and D. B. Nikolov.** 2008. Host cell recognition by the henipaviruses: crystal structures of the Nipah G attachment glycoprotein and its complex with ephrin-B3. Proc. Natl. Acad. Sci. USA **105:**9953–9958.
71. **Yao, Q., X. Hu, and R. W. Compans.** 1997. Association of the parainfluenza virus fusion and hemagglutinin-neuraminidase glycoproteins on cell surfaces. J. Virol. **71:**650–656.
72. **Yin, H.-S., R. G. Paterson, X. Wen, R. A. Lamb, and T. S. Jardetzky.** 2005. Structure of the uncleaved ectodomain of the paramyxovirus (hPIV3) fusion protein. Proc. Natl. Acad. Sci. USA **102:**9288–9293.
73. **Yin, H.-S., X. Wen, R. G. Paterson, R. A. Lamb, and T. S. Jardetzky.** 2006. Structure of the parainfluenza virus 5 F protein in its metastable, prefusion conformation. Nature **439:**38–44.
74. **Yuan, P., G. P. Leser, B. Demeler, R. A. Lamb, and T. S. Jardetzky.** 2008. Domain architecture and oligomerization properties of the paramyxovirus PIV 5 hemagglutinin-neuraminidase (HN) protein. Virology **378:**282–291.
75. **Yuan, P., T. Thompson, B. A. Wurzburg, R. G. Paterson, R. A. Lamb, and T. S. Jardetzky.** 2005. Structural studies of the parainfluenza virius 5 hemagglutinin-neuraminidase tetramer in complex with its receptor, sialyllactose. Structure **13:**1–13.
76. **Yuasa, T., M. Kawano, N. Tabata, M. Nishio, S. Kusagawa, H. Komada, H. Matsumura, Y. Ito, and M. Tsurudome.** 1995. A cell fusion-inhibiting monoclonal antibody binds to the presumed stalk domain of the human parainfluenza type 2 virus hemagglutinin-neuraminidase protein. Virology **206:**1117–1125.